J Mol Model (2011) 17:1579–1586
DOI 10.1007/s00894-010-0842-1

ORIGINAL PAPER

Coupling between the BLUF and EAL domains in the blue light-regulated phosphodiesterase BlrP1

Maria Khrenova · Tatiana Domratcheva · Bella Grigorenko · Alexander Nemukhin

Received: 2 July 2010 / Accepted: 30 August 2010 / Published online: 14 September 2010

Abstract The first biochemical and structural characterization of the full-length active photoreceptor BlrP1 from *Klebsiella pneumoniae* was recently reported by Barends et al. [Nature 459:1015–1018, (2009)]. The light-regulated catalytic function of its C-terminal c-di-guanosine monophosphate phosphodiesterase, the EAL (Glu-Ala-Leu) domain, is activated by the N-terminal sensor of blue light using the flavin adenine dinucleotide (BLUF) domain. We performed molecular dynamics simulations on the dimeric BlrP1 protein in order to examine the coupling regions that are presumably involved in transmitting light-induced structural changes which occur in the BLUF domain to the EAL domain. According to the results of simulations and an analysis of the hydrogen bonding between the respective polypeptide chains, the region containing the site on the α3α4 loop of BLUF is responsible for communication between the photosensing and catalytic domains in the dimeric BlrP1 protein.

M. Khrenova · B. Grigorenko · A. Nemukhin (✉)
Chemistry Department, M.V. Lomonosov Moscow State University,
Leninskie Gory 1/3,
Moscow 119991, Russian Federation
e-mail: anemukhin@yahoo.com

A. Nemukhin
e-mail: anem@lcc.chem.msu.ru

T. Domratcheva
Department of Biomolecular Mechanisms,
Max Planck Institute for Medical Research,
69120 Heidelberg, Germany

A. Nemukhin
N.M. Emanuel Institute of Biochemical Physics,
Russian Academy of Sciences,
Kosygina 4,
Moscow 119334, Russian Federation

Keywords Photoreceptor protein BlrP1 · Signal transduction · Photosensing BLUF domain · Catalytic EAL domain · Hydrogen bonding · Molecular dynamics

Introduction

Numerous cellular functions are regulated by extracellular stimulation through alterations of intracellular cyclic nucleotide levels. In particular, the activity of phosphodiesterases (PDE)—enzymes that catalyze the degradation of cyclic nucleotides—is tightly regulated with respect to different environmental conditions. Accordingly, the enzymatic domains are often found on the same polypeptide chain as the signal-sensing and regulatory domains. Such modular protein organization allows the control of enzymatic activity with respect to various stimuli.

Cyclic dimeric guanosine monophosphate, c-di-GMP, is a bacterial global secondary messenger that is implicated in a variety of cellular functions, including virulence expression and biofilm formation. Biochemical studies have linked the specific activity of c-di-GMP phosphodiestarase to proteins that contain EAL domains. Named after the conserved amino acid signature motif Glu-Ala-Leu, EAL is a metal-dependent phosphodiestrase that catalyzes the hydrolysis of c-di-GMP into the linear nucleotide 5′-pGpG [1–10]. In the phosphodiesterase BlrP1 from *Klebsiella pneumoniae*, the catalytic function of the C-terminal EAL domain is regulated by the N-terminal sensor of blue light-using flavin adenine dinucleotide (BLUF). The first biochemical and structural characterization of the full-length blue light-activated phosphodiesterase BlrP1 from *Klebsiella pneumoniae* was recently reported [11]. The PDE activity of BlrP1 was found to increase fourfold upon light illumination.

The BLUF domains constitute a recently discovered class of flavin-binging photoreceptors that are implicated in various light responses in bacteria. Several BLUF-containing proteins from different organisms have been extensively studied [12–24]; nonetheless, the mechanism of BLUF light sensing is still the focus of considerable debate. BLUF domains have a ferredoxine-like folded core capped by a helical extension. Photon absorption by the flavin chromophore induces hydrogen bond rearrangement in the core of the domain, resulting in the formation of the light-activated state. Based on crystal structures [14, 15], a putative light-induced conformation switch involving the β_5 strand and the loop connecting β_4 and β_5 was discussed in the literature. Signal transduction via the linked BLUF and EAL $\alpha_3\alpha_4$ helices was proposed for the YcgF photoreceptor, a protein homologous to BlrP1 in *Escherichia coli* [23]. In addition, in an NMR study of the BLUF domain from BlrP1 [24], structural changes occurring up to 15 Å from the chromophore in the $\alpha_3\alpha_4$ helical cap were observed upon progressing from the dark to the light state. Hence, Wu and Gardner [24] distinguished the following sites of BlrP1-BLUF which may undergo significant light-induced changes: the $\beta_4\beta_5$ loop, the $\alpha_3\alpha_4$ loop and the β_5 strand.

According to crystal structures [11], the EAL domain adapts a TIM-barrel fold. BlrP1 forms an antiparallel dimer with the interface created by the EAL α_5 and α_6 helices (termed "compound" and "dimerization" helices, respectively). The BLUF domains are packed against the EAL–EAL dimer interface such that the EAL and BLUF domains of the different monomers form close contacts in several regions. In the mechanism of light-regulated enzymatic activity in BlrP1 hypothesized by Barends et al. [11], the light-induced changes in the BLUF domain of one monomer are transmitted via the dimerization interface to the active site of the EAL domain of the other monomer. It should be noted that the interfaces aBLUF–bEAL and bBLUF–aEAL are not structurally and dynamically identical.

In this work we used methods of molecular modeling to examine prospective coupling regions that may be involved in transmitting light-induced structural changes from the BLUF domain to the EAL domain in the light-activated phosphodiesterase BlrP1. An analysis of the hydrogen bonding in these regions following molecular dynamics simulations on the dimeric BlrP1 protein allowed us to distinguish a specific site that is responsible for communication between the photosensing and catalytic domains.

Computational protocol

Calculations of MD trajectories were performed using the NAMD 2.6 software suite [25] which is freely available at http://www.ks.uiuc.edu/Research/namd/. The CHARMM22 force field parameters (http://mackerell.umaryland.edu/CHARMM_ff_params.html) for protein atoms and Mg^{2+}, the CHARMM27 force field parameters for c-di-GMP and the TIP3P model parameters for all water molecules were employed. The GAFF force field parameters [26, 27] were used for FMN. Starting structures were generated from the 2.55 Å-resolution crystal structure of the *Klebsiella pneumoniae* BlrP1 protein (Protein Data Bank entry 3GG0 [11]). Since some of the residues were absent in the PDB structure, we re-constructed certain parts of the protein, namely residues 115–119 in the α3α4 loop of monomer b, taking them from monomer a of the same structure and a part of the loop connecting the BLUF and EAL domains (residues 155–157 from monomer b and 154–159 from monomer a).

The protein was solvated in a rectangular box of TIP3P water molecules of size 103 × 106 × 100 $Å^3$, and the charge was neutralized by adding 18 ions. Periodic boundary conditions were assumed. All long-range electrostatic interactions were computed using the particle mesh Ewald method [25]. Constant-temperature MD simulations were performed for the NVT ensemble at 300 K using the Langevin thermostat. The simulations were carried out with a 1 fs integration step following a 1500-step energy minimization. No restrictions were imposed on the coordinates of the atoms in the trajectory calculations. The VMD program [28] was used for visualization (http://www.ks.uiuc.edu/Research/vmd/).

MD calculations and energy minimization for a protein in a water box may be problematic due to the physical density relating to artificial cavities in water shells. In order to avoid problems with inconsistent densities, we performed MD simulations under NPT ensemble conditions at the preliminary stages of the project. The computed density in our model system was 1.08 g/cm^3.

Three separate 5 ns trajectories were selected for an analysis of hydrogen bonding in the dimeric protein. We verified that a fairly lengthy trajectory of up to 20 ns resulted in the same qualitative conclusions as a more economical 5 ns run. The data presented in Table 1 compare the stabilities of hydrogen bonds for selected pairs of amino acids computed with trajectories of 5 ns and 20 ns using the distance criterion or the distance and angle criteria. The stability of a hydrogen bond is the percentage of time that the bond is formed; a value which is close to 100% indicates that the hydrogen bond between two amino acid residues is stable.

It is clear that reducing the trajectory from 20 ns to 5 ns does not introduce crude mistakes into the qualitative conclusions, which are the main aim of this work. Although the stabilities of a few hydrogen bonds appeared to be different in the 5 ns and 20 ns trajectories, e.g., those for Thr118N–Asp267Oδ2 (93% vs 60%) and Arg138Nη2–

Table 1 Stability of hydrogen bonds between pairs of amino acids from the BLUF and EAL domains as computed using trajectories of 5 ns and 20 ns. The distance between the heavy donor and acceptor atoms D…A (denoted *R*) and the angle D–H…A (denoted Φ) can be considered the parameters that define the occurrence of the hydrogen bond

Hydrogen bonds between bBLUF and aEAL	Stability (%)					
	5 ns trajectory			20 ns trajectory		
	R<3.2 Å	*R*<3.2 Å and 90°<Φ <180 °	*R*<3.2 Å and 150°<Φ <180 °	*R*<3.2 Å	*R*<3.2 Å and 90°<Φ <180 °	*R*<3.2 Å and 150°<Φ <180 °
Val117N–Asp267Oδ1	19.5	19.5	17.5	9.7	9.7	8.6
Val117N–Asp267Oδ2	53.7	53.7	6.4	33.0	32.9	4.9
Thr118N–Asp267Oδ2	93.2	93.2	84.9	59.8	59.8	55.1
Thr118Oγ–Asp267Oδ2	99.8	99.8	94.8	64.4	64.2	59.9
Asn122Oδ1–Lys321Nζ	68.1	68.1	4.8	68.1	68.1	9.6
Arg127Nη2–Asp320Oδ1	99.2	99.2	92.8	96.6	96.6	73.6
Arg127Nη2–Gly353O	85.3	85.3	18.3	93.5	93.6	49.3
Arg127Nε–Gly353O	98.0	98.0	67.3	70.6	70.6	36.2
Arg124Nε–Leu352O	99.6	99.6	72.1	99.5	99.5	71.0
Arg124Nη2–Leu352O	75.7	75.7	25.1	70.7	70.7	17.5
Arg138Nη2–Asp351Oδ1	92.0	92.0	86.9	63.2	63.2	55.6
Arg138Nη2–Asp351Oδ2	11.6	11.6	3.6	43.4	43.4	33.6
Arg138Nη1–Glu350Oε1	60.6	60.6	44.6	49.2	49.2	35.7
Arg138Nη1–Glu350Oε2	39.4	39.4	27.1	47.9	47.9	30.8

Asp351Oδ1 (92% vs 63%), these differences do not affect the qualitative results: in both cases we classify these hydrogen bonds as being stable ones.

We also analyzed the sensitivity of the results to the criteria used for hydrogen bond formation. Several geometry-based empirical rules of hydrogen bond identification have been proposed in the literature [29–32]. In particular, the distance between the heavy donor and acceptor atoms D…A (denoted in Table 1 as *R*) and the angle D–H…A (denoted as Φ) may be considered the primary parameters that define the occurrence of the hydrogen bond. D–H…A bond linearity is not strictly required for amino acid residues, especially when Lys is considered. In [29], distances *R* of less than 3.9 Å and angles Φ of between 90° and 180° are allowed for hydrogen bond formation. In Table 1, the three columns furthest to the right show hydrogen bond stabilities computed with the different hydrogen bond occurrence criteria. The requirement for an almost linear angle 150°<Φ<180° formally reduces the number of hydrogen bonds; however, in many cases, visual inspection of the hydrogen bond network shows that the less strict requirement 90°<Φ<180° is more accurate [29]. Therefore, we rely on the distance criterion *R*<3.2 Å and on 5 ns trajectories in the results discussed below. We stress that our goal was to compare different regions of the dimeric protein with respect to hydrogen bond formation, based on the same level of assignment of hydrogen bonds.

Results and discussion

Careful inspection of the crystal structure PDBID: 3GG0 [11] shows that three particular regions, as illustrated in Fig. 1, can be expected to undergo changes when the system proceeds from the dark state to the light-activated state. We distinguish the following contacts at both BLUF–EAL interfaces:

(i) Between the BLUF domain α3α4 loop (residues 114–123) and the EAL domain α3′β4 loop (residues 262–268), designated the "α3α4 loop contact" (left panel in Fig. 1)

(ii) Between the BLUF domain α4 helix (residues 122–138) and the EAL β6 sheet (residues 320–324) and the so-called α6′β7 connector loop (residues 350–354), designated the "α4 helix contact" (right panel in Fig. 1)

(iii) Between the BLUF domain β4β5 loop (residues 83–92) and the EAL domain α3′β4 loop (residues 262–268) and the α4′β5 loop (residues 295–297) designated the "β4β5 loop contact" (central panel in Fig. 1).

For each region, we monitored the stabilities of the hydrogen bonds between the pairs of residues from the BLUF and EAL domains along the MD trajectories by relying on the following criterion: a hydrogen bond is assumed to be formed if the distance between the heavy

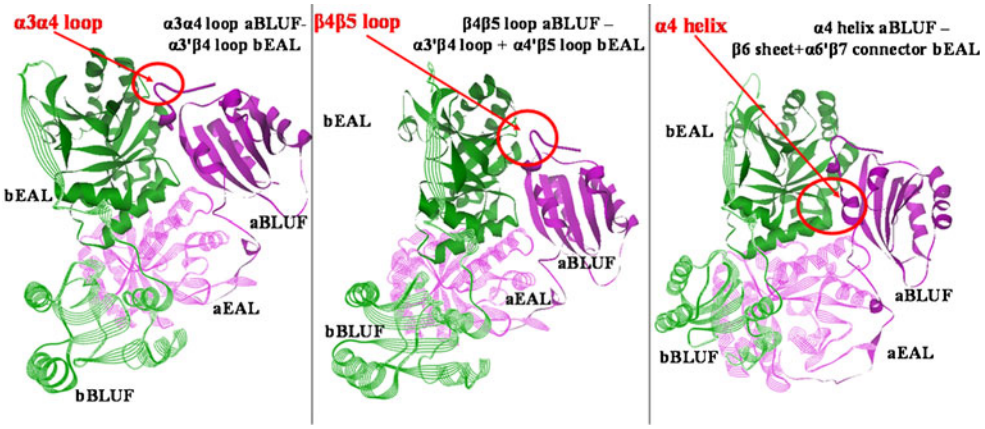

Fig. 1 Three regions that presumably mediate BLUF–EAL coupling in the BlrP1 dimer. The *flat ribbon* presentation distinguishes the aBLUF–bEAL pair, while the *line ribbon* presentation refers to the other pair, bBLUF–aEAL. In all of the figures included in this paper, we use *purple* to distinguish monomer a and *green* to show monomer b of the dimeric BlrP1 protein a(BLUF…EAL)–b (BLUF…EAL)

atoms does not exceed 3.2 Å, as discussed in the preceding section. Recall that the stability of a hydrogen bond is defined here as the percentage of time that the bond is formed; a value which is close to 100% indicates that the hydrogen bond between two amino acid residues is stable. The computed values for the selected EAL–BLUF regions are collected in Table 2.

Before we proceed to discuss the hydrogen bonding in the BLUF–EAL coupling regions, it is important to note that there are only a few hydrogen bonds that contribute to the EAL–EAL dimer interface. According to the applied criterion, the hydrogen bond between Oγ in Ser344 from aEAL and the oxygen atom of the polypeptide backbone of Ser344 from bEAL and vice versa possess stabilities of around 50%. For half of the simulation time those bonds are broken and replaced by hydrogen bonds with the backbone oxygen atom of Ala340 from the same monomer. On the other hand, fairly stable hydrogen bonds between Arg138 from one monomer and Asp351 and Glu350 from the other monomer may account for the specific orientation

Table 2 Stabilities of the hydrogen bonds between pairs of amino acids from the BLUF and EAL domains during MD simulations with 5 ns trajectories. The values obtained from trajectories 1, 2, and 3 are shown in different columns. An empty cell implies that the value is less than 5%

Contact	Hydrogen bonds between aBLUF and bEAL	Stability (%)			Hydrogen bonds between bBLUF and aEAL	Stability (%)		
		1	2	3		1	2	3
α3α4 loop	Val117N–Asp267Oδ1		10.0		Val117N–Asp267Oδ1	15.6	11.4	24.8
	Val117N–Asp267Oδ2	11.2	84.2	6.2	Val117N–Asp267Oδ2	86.4	75.4	56.5
	Thr118N–Asp267Oδ2	13.4	95.4	9.2	Thr118N–Asp267Oδ2	94.2	89.0	93.9
	Thr118Oγ–Asp267Oδ1	55.8			Thr118Oγ–Asp267Oδ1			
	Thr118Oγ–Asp267Oδ2	16.2	99.2	22.2	Thr118Oγ–Asp267Oδ2	99.4	94.0	99.7
α4 helix	Asn122Oδ1–Lys321Nδ	95.4	95.0	90.3	Asn122Oδ1–Lys321NZ	92.4	94.4	70.2
	Arg127Nη2–Asp320Oδ1				Arg127Nη2–Asp320Oδ1	98.4	87.6	99.2
	Arg127Nη2–Gly353O				Arg127Nη2–Gly353O	92.2	81.0	85.0
	Arg127Nη1–Gly353O				Arg127Nε–Gly353O	98.0	97.4	96.3
	Arg127Nη1–Thr355Oγ				Arg127Nδ1–Thr355Oγ			70.0
	Arg127Nε–Thr355Oγ	58.4			Arg127Nε–Thr355Oγ			
	Arg124Nε–Leu352O	94.2	97.6	96.8	Arg124Nε–Leu352O	94.4	85.6	99.2
	Arg124Nη2–Leu352O	79.4	78.8	85.9	Arg124Nη2–Leu352O	79.4	92.0	79.3
	Arg138Nδ1–Asp351Oδ1		90.0	8.3	Arg138Nη2–Asp351Oδ1	99.8	86.4	99.8
	Arg138Nδ1–Asp351Oδ2		37.2		Arg138Nε–Asp351Oδ2			
	Arg138Nε–Asp351Oδ1	17.2	60.8	5.8	Arg138Nε–Asp351Oδ1			
	Arg138Nε–Asp351Oδ2	62.2	15.2	8.1	Arg138Nε–Asp351Oδ2			
	Arg138Nη1–Glu350Oε1	25.0			Arg138Nη1–Glu350Oε1	59.6	73.8	52.1
	Arg138Nη1–Glu350Oε2	68.0	32.0		Arg138Nη1–Glu350Oε2	8.2	31.0	39.8
β4β5 loop	Tyr84OH–Gly296O				Tyr84OH–Gly296O	25.8	21.8	60.4
	Tyr84OH–Lys298Nζ	8.0		32.0	Tyr84OH–Lys298Nζ	38.0	25.8	8.4

of the dimerization helices at the EAL–EAL interface. The hydrogen bonds with Arg138 contribute to the α4 helix contact described below.

(i) The α3α4 loop contact

Figure 2 and data in Table 1 show hydrogen-bonding interactions of the α3α4 loop of BLUF with the α3′β4 loop of EAL. In particular, the carboxylate group of Asp267 from EAL forms stable hydrogen bonds with the protein backbones of both Val117 and Thr118 and with the hydroxyl group of Thr118 from BLUF in the aBLUF–bEAL pair. In EAL, the conformational change in the α3′β4 loop may be transmitted via the β4 strand to the α4 helix, the structural arrangement of which was considered to be critical for catalytic activity [11]. The β4 strand contains the residue Glu272 which coordinates the catalytic metal ion. Further, residue Glu275, situated at the N-terminus of the α4 helix, was proposed to be involved in allosteric regulation of the PDE activity [10, 33]. Assuming that signal transduction after the activation of the flavin chromophore by light proceeds towards the α3α4 loop in BLUF, the strong hydrogen bonding with the α3′β4 loop of the EAL partner mediates the described conformational change in EAL.

The results for the other pair, bBLUF–aEAL, presented in the columns on the right of Table 1, demonstrate less stable hydrogen bonding between Thr118 and Asp267, which can be attributed to the specific features of the model system. Residues 115–119 of the bBLUF domain are missing in the crystal structure PDBID: 3GG0, which indicates that this region has increased structural flexibility. Therefore, we reconstructed the missing 115–119 residues manually by taking the corresponding peptide fraction from the other monomer for the MD simulations.

(ii) The α4 helix contact

Figures 3 and 4 and data in Table 1 illustrate the hydrogen bonding in this contact region. Arg124 and Arg127 are the principal partners from the BLUF α4 helix, while the residues Leu352 and Gly353 from the loop adjacent to the connector helix from EAL serve as suitable counterparts. The hydrogen bonds that are formed by Arg124 with Leu352 are stable in both pairs, aBLUF–bEAL and bBLUF–aEAL. In contrast, due to the noticeably different orientations of the Arg127 side chain in the monomers, its hydrogen bonding is less pronounced. The side chain Arg127 in aBLUF is firmly fixed between the β6 and β7 sheets and its hydrogen bonds with Asp320 and Gly353 from bEAL are stable for the entire simulation time (Table 1). The hydrogen bond between Arg127 from bBLUF and Thr355 from aEAL is stable for only the first half of the simulation time. The bond is then cleaved and Arg127 adopts a solvent-exposed conformation.

Figure 4 shows other interactions between the residues from the EAL domain and those from the α4 helix of BLUF. Residue Asp123 interacts with residue Lys298 via a stable hydrogen bond in both pairs, aBLUF–bEAL and bBLUF–aEAL (not shown in Table 1). Other hydrogen bonds presented in Fig. 4 are characterized in Table 1. The side chain of Lys321 in both monomers changes its orientation considerably along the MD trajectories (with

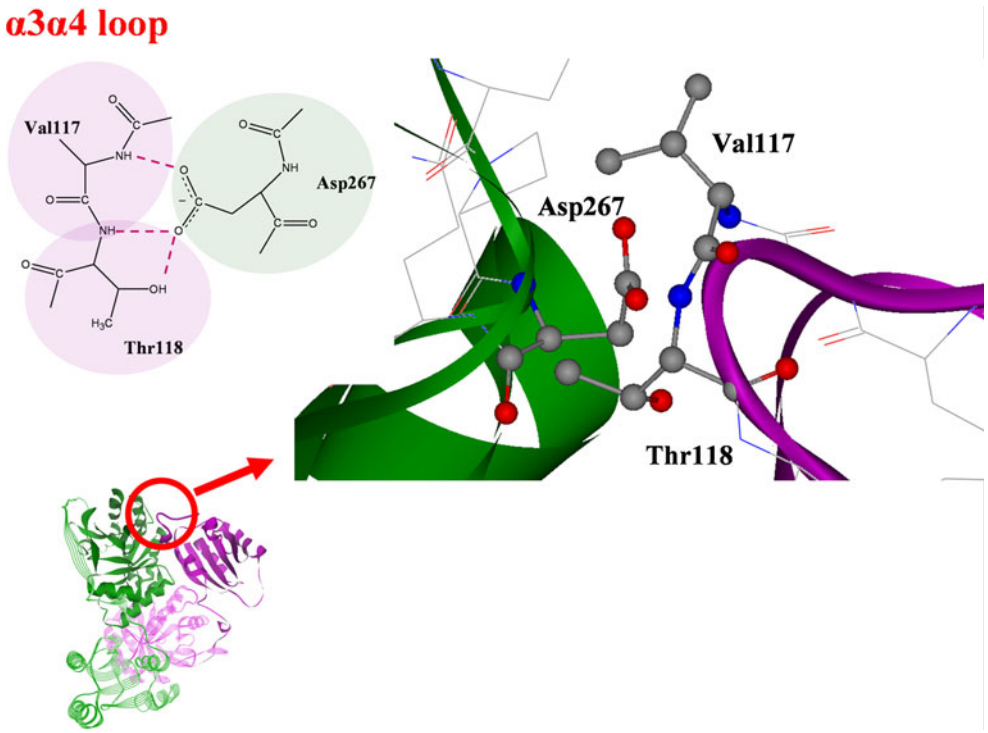

Fig. 2 Hydrogen-bonding interactions of the α3α4 loop contact

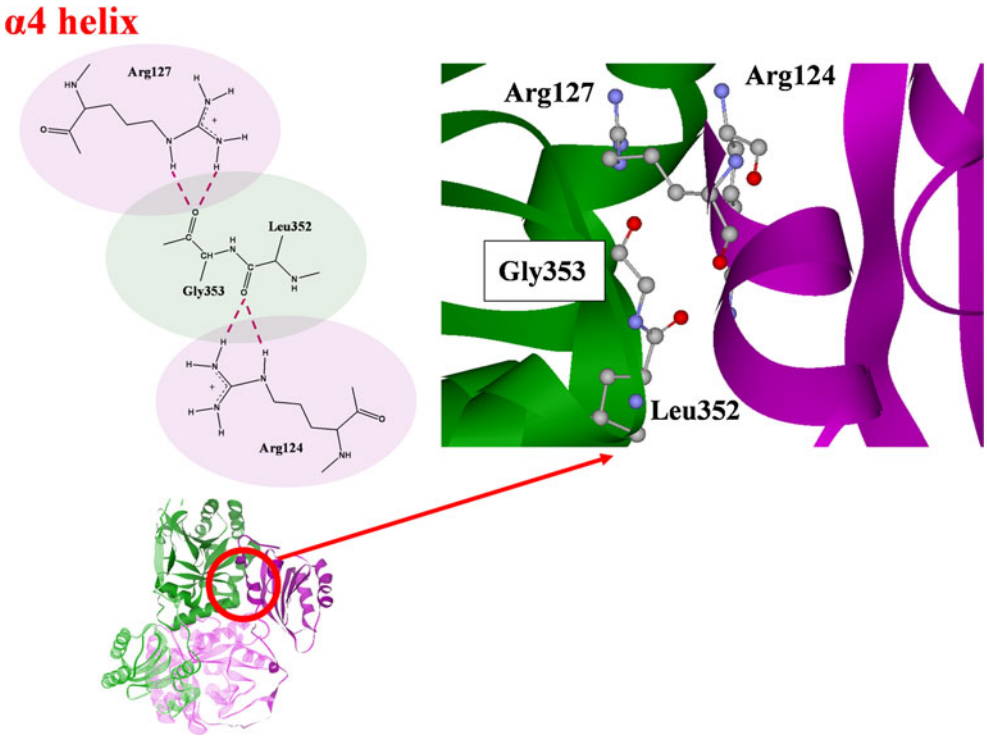

Fig. 3 Hydrogen-bonding interactions of Arg124 and Arg127 from the α4 helix contact region

the most prominent changes occurring within first 200 ps). We note that this is the only case where the conformations observed as a result of MD simulations differ considerably from the parent crystal structure. During the course of simulations, stable Lys321–Asn122 hydrogen bonds are formed, which are not observed in the crystal structures. In addition, the Arg138 located immediately after the α4 helix of BLUF forms hydrogen bonds with Glu350 and Asp351. These hydrogen bonds further contribute to the protein–protein binding mediated by this contact region.

To sum up, in this contact region we see that interactions of the BLUF α4 helix with the EAL domain of the other monomer include multiple stable hydrogen bonds. To induce noticeable changes in the EAL domain through the

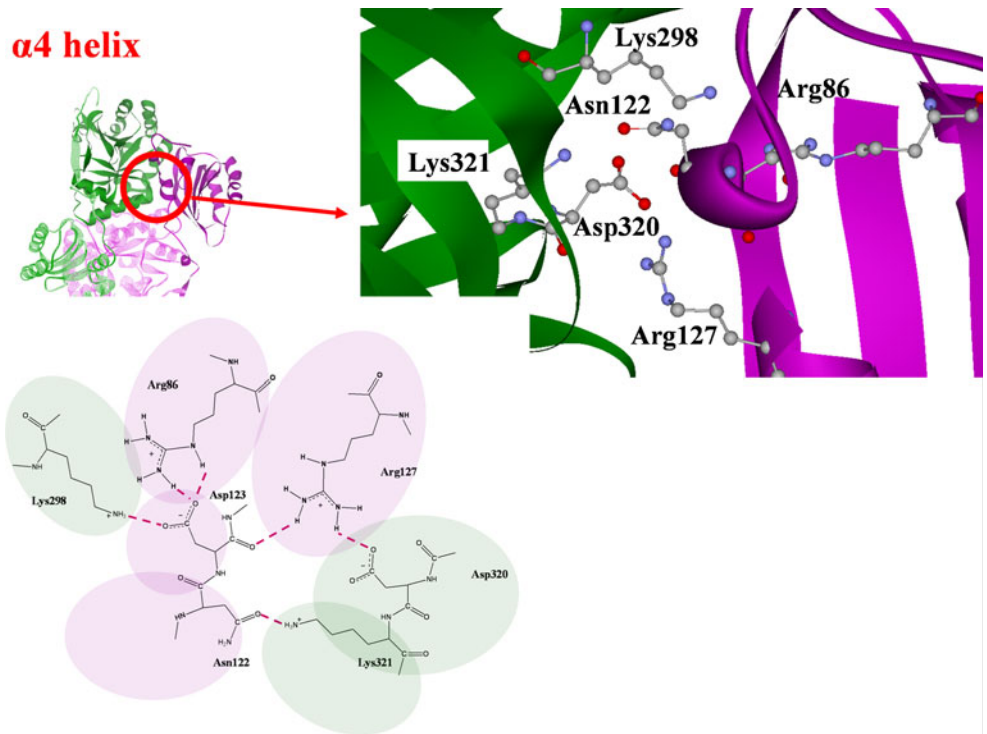

Fig. 4 Hydrogen-bonding interactions of Asp123 and Asp320 from the α4 helix contact region

light activation of BLUF, too many hydrogen-bonded pairs of amino acid side chains would need to be affected simultaneously. Therefore, this region is unlikely to be involved in transmitting light-induced structural changes in the BLUF domain to the EAL domain. We suggest that this area could be responsible for the specific orientations of the BLUF domains with respect to the EAL domains in the dimer.

(iii) The β4β5 loop contact

The β4β5 loop in BLUF has been proposed to mediate signal transduction to EAL, since light-induced changes have been considered in this area for the BLUF domain of another blue-light sensing protein, AppA [14, 15, 20]. The proposed light-induced structural change involves a two-residue shift in the β5 strand relative to the surrounding β sheet, shortening the β4β5 loop. This change is linked to the conformations of the conserved Met residue from the β5 strand and the Trp residue from the β4β5 loop in AppA. Although the BLUF domains in BlrP1 do not possess Trp residues analogous to that in AppA, we can assume that similar transformations could take place with Met92 from the β5 strand in BlrP1. Discouragingly, our MD simulations show (Table 1) that the β4β5 loop in the BLUF domains of BrlP1 is not involved in pronounced hydrogen bonding with the EAL domains. The only candidate that forms a hydrogen bond is the side chain of Tyr84. However, according to the MD simulations, Tyr84 tends to form hydrogen bonds with the side chains of the same BLUF domain (Phe115 and Asp123) or with solvating water molecules. As such, we conclude that this region is unlikely to be responsible for the light sensitivity of BlrP1.

Conclusions

Monitoring the stabilities of the hydrogen bonds that mediate the BLUF–EAL interactions leads us to propose the following roles for the prospective contact regions. The α3α4 loop of BLUF that interacts with the α3′β4 loop of EAL is implicated in the acceleration of the reaction in the light-induced state. This pathway is consistent with the results of NMR studies of the BLUF domain of BlrP1 [24], which indicate that the most significant changes upon the formation of the light-induced state are those for the α3α4 loop of BLUF. Moreover, the most pronounced minimum chemical shift differences in the $^{15}N/^{1}H$ HSQC spectra [24] were assigned to Val117 and Thr118. These residues, as our MD simulations indicate (Table 1), form stable hydrogen bonds with Asp267 from the EAL domain. Therefore, we conclude that the light-induced structural changes in the contact region formed by the BLUF α3α4 loop and the EAL α3′β4 loop are responsible for the acceleration of the reaction in the light-induced state of BlrP1. The region formed by the α4 helix of BLUF and the β6 sheet and α6′β7 connector of EAL accounts for the specific BLUF–EAL binding. The β4β5 loop of BLUF is barely involved in hydrogen-bonding interactions with the nearby α3′β4 and α4′β5 loops of EAL; therefore, this contact does not contribute to BLUF–EAL functional coupling.

Acknowledgments We are very grateful to Dr. Ilme Schlichting for helpful discussions. This work was supported in part by grants from the Deutsche Forschungsgemeinschaft FOR526 and from the Russian Foundation for Basic Research (project no. 10-03-00139). The Russian team is grateful for the use of the facilities of the supercomputing complex of the Research Computing Center of M.V. Lomonosov Moscow State University and the SKIF-GRID program for providing computational resources.

References

1. Jenal U, Malone J (2006) Annu Rev Genet 40:385–407
2. Tarutina M, Ryjenkov DA, Gomelsky M (2006) J Biol Chem 281:34751–34758
3. Römling U, Amikam D (2006) Curr Opin Microbiol 9:218–228
4. Cotter PA, Stibitz S (2007) Curr Opin Microbiol 10:17–23
5. Römling U, Gomelsky M, Galperin MY (2007) Mol Microbiol 57:629–639
6. Hisert KB, MacCoss M, Shiloh MU, Darwin KH, Singh S, Jones RA, Ehrt S, Zhang Z, Gaffney BL, Gandotra S, Holden DW, Murray D, Nathan C (2005) Mol Microbiol 56:1234–1245
7. Hoffman LR, D'Argenio DA, MacCoss MJ, Zhang Z, Jones RA, Miller SI (2005) Nature 436:1171–1175
8. Kulasakara H, Lee V, Brencic A, Liberati N, Urbach J, Miyata S, Lee DG, Neely AN, Hyodo M, Hayakawa Y, Ausubel FM, Lory S (2006) Proc Natl Acad Sci USA 103:2839–2844
9. Schmidt AJ, Ryjenkov DA, Gomelsky M (2005) J Bacteriol 187:4774–4781
10. Rao F, Yang Y, Qi Y, Liang Z-X (2008) J Bacteriol 190:3622–3631
11. Barends TR, Hartmann E, Griese JJ, Beitlich T, Kirienko NV, Ryjenkov DA, Reinstein J, Shoeman RL, Gomelsky M, Schlichting I (2009) Nature 459:1015–1018
12. Gomelsky M, Klug G (2002) Trends Biochem Sci 27:497–500
13. Jung A, Domratcheva T, Tarutina M, Wu Q, Ko W-H, Shoeman RL, Gomelsky M, Gardner KH, Schlichting I (2005) Proc Natl Acad Sci USA 102:12350–12355
14. Jung A, Reinstein J, Domratcheva T, Shoeman RL, Schlichting I (2006) J Mol Biol 362:717–732
15. Anderson S, Dragnea V, Masuda S, Ybe J, Moffat K, Bauer C (2005) Biochemistry 44:7998–8005
16. Kita A, Okajima K, Morimoto Y, Ikeuchi M, Miki K (2005) J Mol Biol 349:1–9
17. Yuan H, Anderson S, Masuda S, Dragnea V, Moffat K, Bauer C (2006) Biochemistry 45:12687–12694
18. Tyagi A, Penzkofer A, Griese J, Schlichting I, Kirienko NV, Gomelsky M (2008) Chem Phys 354:130–141
19. Gomelsky M, Kaplan S (1998) J Biol Chem 273:35319–35325
20. Domratcheva T, Grigorenko BL, Schlichting I, Nemukhin AV (2008) Biophys J 94:3872–3879

21. Gauden M, van Stokkum IH, Key JM, Lührs DC, van Grondelle R, Hegemann P, Kennis JT (2006) Proc Natl Acad Sci USA 103:10895–10900
22. Wu Q, Ko WH, Gardner KH (2008) Biochemistry 47:10271–10280
23. Schroeder C, Werner K, Otten H, Krätzig S, Schwalbe H, Essen L-O (2008) ChemBioChem 9:2463–2473
24. Wu Q, Gardner KH (2009) Biochemistry 48:2620–2629
25. Phillips JC, Braun R, Wang W, Gumbart J, Tajkhorshid E, Villa E, Chipot C, Skeel RD, Kale L, Schulten K (2005) J Comput Chem 26:1781–1802
26. Wang J, Wang W, Kollman PA, Case DA (2006) J Mol Graphics 25:247–260
27. Wang J, Wolf RM, Caldwell JW, Kollman PA, Case DA (2004) J Comput Chem 25:1157–1174
28. Humphrey W, Dalke A, Schulten K (1996) J Molec Graphics 14:33–38
29. McDonald IK, Thornton JM (1994) J Mol Biol 238:777–793
30. Torshin IY, Weber IT, Harrison RW (2002) Protein Eng 15:359–363
31. Fabiola F, Bertran R, Korostelev A, Chapman MS (2002) Protein Sci 11:1415–1423
32. Aakeröy KB, Evans TA, Seddon KR, Pálinkó I (1999) New J Chem 23:145–152
33. Rao F, Qi Y, Chong HS, Kotaka M, Li B, Li J, Lescar J, Tang K, Liang Z-X (2009) J Bacteriol 191:4722–4731